

1 **The contribution of carbon and water in modulating wood formation in black**
2 **spruce saplings**

3 **Annie Deslauriers¹, Jian-Guo Huang^{2,3,1*}, Lorena Balducci¹, Marilène Beaulieu¹, Sergio**
4 **Rossi^{1,2}**

5 ¹Département des Sciences Fondamentales, Université du Québec à Chicoutimi, 555 boulevard
6 de l'Université, Chicoutimi, QC G7H2B1, Canada.

7 ²Key Laboratory of Vegetation Restoration and Management of Degraded Ecosystems, South
8 China Botanical Garden, Chinese Academy of Sciences, Guangzhou 510650, China

9 ³Provincial Key Laboratory of Applied Botany, South China Botanical Garden, Chinese
10 Academy of Sciences, Guangzhou 510650, China

11 **One sentence summary:** During wood formation, water availability is the most important factor
12 for cell production while carbon is more important to sustain the differentiation of the living
13 cells.

14 **Funding information:** This study was funded by the Natural Sciences and Engineering
15 Research Council of Canada (Discovery Grant of A. Deslauriers), MITACS grant of JG Huang
16 and the Consortium Ouranos. JG Huang was also funded by the 100 Talents Program of the
17 Chinese Academy of Sciences (No.Y421081001) and the National Natural Science Foundation
18 of China (No.31570584).

19 ***Corresponding author:** Jian-Guo Huang, Key Laboratory of Vegetation Restoration and
20 Management of Degraded Ecosystems, Provincial Key Laboratory of Applied Botany, South

21 China Botanical Garden, Chinese Academy of Sciences, Guangzhou 510650, China E-
22 mail:huangjg@scbg.ac.cn, telephone +86 20-37264225, fax +86 20-37264153

23 **Summary**

24 Non-structural carbohydrates (NSCs) play a crucial role in xylem formation and represent, with
25 water, the main constraint to plant growth. We assessed the relationships between xylogenesis
26 and NSCs in order to (1) verify the variance explained by NSCs and (2) determine the influence
27 of intrinsic (tissue supplying carbon) and extrinsic (water availability and temperature) factors.
28 During two years, wood formation was monitored in saplings of black spruce submitted to a dry
29 period of about one month in June and exposed to different temperature treatments in a
30 greenhouse. In parallel, NSCs concentrations were determined by extracting the sugar
31 compounds from two tissues (cambium and inner xylem), both potentially supplying carbon for
32 wood formation. A mixed-effect model was used to assess and quantify the potential
33 relationships. Total xylem cells, illustrating meristematic activity, were modeled as a function of
34 water, sucrose and pinitol (conditional R^2 of 0.79). Water availability was ranked as the most
35 important factor explaining total xylem cell production, while the contribution of carbon was
36 lower. Cambium stopped dividing under water deficit, probably to limit the number of cells
37 remaining in differentiation without an adequate amount of water. By contrast, carbon factors
38 were ranked as the most important in explaining the variation in the living cells (conditional R^2
39 of 0.49) highlighting the functional needs during xylem development, followed by the tissue
40 supplying the NSCs (cambium) and water availability. This study precisely demonstrates the role
41 of carbon and water in structural growth expressed as meristematic activity and tissue formation.

42 **Keywords:** Cambium, cell enlargement, cell wall thickening, drought, temperature, non-
43 structural soluble sugars, source-sink relationships

INTRODUCTION

44

45 Mobile sugars (e.g. sucrose, glucose and fructose) and sugar alcohols (e.g. pinitol) play an
46 essential role in sustaining plant growth and metabolism and plant signaling (Muller et al., 2011).
47 The origin of non-structural carbohydrates (NSCs) (reserve *versus* recent photosynthetic
48 products) and their importance for growth processes are currently under intensive investigation
49 (Wiley and Helliker, 2012; Rocha, 2013). The C-incorporation during wood formation, mostly in
50 the form of cellulose and other cell wall polymers, determines most of the biomass accumulated
51 by trees. In red maple, the NSC used to build the xylem is less than 1-yr-old (Carbone et al.,
52 2013), demonstrating a fast incorporation of C originating from the mobile sugars pool in the
53 stem. Reserves are often used at growth resumption in early spring (Oribe et al., 2003; Begum et
54 al., 2013), but most xylem is formed with newly synthesized NSCs (Hansen and Beck, 1990,
55 1994; Kagawa et al., 2006). The ray parenchyma cells in xylem could also act as a source of
56 NSCs to sustain growth when assimilates coming from the leaf become scarce (Maunoury-
57 Danger et al., 2010; Olano et al., 2013) such as during a water deficit. As the molecular networks
58 driving cell division and expansion largely rely on the availability of carbohydrates to provide
59 energy and biomass (Lastdrager et al., 2014), xylem formation is an ideal system to study source-
60 sink relationships and C-dependence of the growth metabolism.

61 The cambium is the meristem that produces layers of phloem and xylem cells in stem, branches
62 and roots with a periodic activity that results in the seasonal radial growth (Rossi et al., 2013).

63 The machinery of growth requires C-resources for many processes, in particular to supply energy
64 for division, generate water turgor pressure during cell expansion, and produce polysaccharides
65 during cell-wall formation (Muller et al., 2011). Recent evidence strongly supports the
66 association between the pattern of NSCs and wood formation: the rate of xylem growth follows

67 the concentration of NSCs in cambium, reflecting the strong demand for C-compounds in the
68 phases of cell enlargement and cell-wall thickening (Deslauriers et al., 2009; Simard et al.,
69 2013). Specific carbon compounds are needed according to the stage of wood development:
70 increases in volume during cell expansion (i.e. cell growth) need osmotically active C-
71 compounds and water to generate a suitable wall-yielding turgor pressure in growing cells
72 (Steppe et al., 2015) while cell maturation needs C-compounds as substrate to build cell walls
73 (Koch, 2004). The mobile pool of sugars allocated to growing and differentiating cells thus
74 represents a direct constraint to wood formation (Michelot et al., 2012; Simard et al., 2013). Two
75 nearby mobile carbohydrate pools can directly sustain wood formation: cambium – assuming
76 that the C-compound comes from sucrose unloaded from phloem, and xylem – assuming that the
77 C-compound comes from ray parenchyma (Deslauriers et al., 2009; Giovannelli et al., 2011). A
78 relationship between the forming xylem and the available soluble sugars in each pool could
79 therefore significantly improve our understanding of the use of NSCs in secondary growth and
80 the importance of their provenance (current photosynthesis versus reserve). Compared with the
81 outermost xylem, much higher amounts of NSCs are found in cambium (Deslauriers et al., 2009;
82 Simard et al., 2013) because of its proximity to the unloading sites in phloem.

83 In the absence of water deficit, correlations are reported between the growth of various organs
84 and C-availability (in roots, young leaves, flowers, fruits and seeds), but these relationships can
85 be modified or reduced under stress [see review by Muller et al. (2011) and Tardieu et al.
86 (2011)]. Drought-related growth reductions are primarily caused by hydromechanical constraints
87 rather than C-availability (Pantin et al., 2013; Steppe et al., 2015), which could explain the
88 uncoupling between NSCs and cell growth. Characterization of the interacting role of C and

89 water availability in xylem cell differentiation is therefore needed, as well as the main source of
90 carbon for wood formation.

91 The objectives of this study were (1) to verify the relationships between xylem production and
92 available NSCs and (2) to determine the influence of tissue supplying NSCs, water availability
93 and temperature. In the study, xylem production was characterized by the living cells – the sum
94 of the number of cells in cambium (C), enlargement (ENL) and cell wall thickening (CWT) –
95 representing the cells with high metabolic activity, and by the total number of xylem cells
96 formed – differentiating and mature cells – representing the sum of tree-ring growth during the
97 growing season (Figure 1). The tissue supplying carbon represents the NSCs coming from
98 cambium or the inner xylem (Figure 1). In relation to the objectives, we considered the
99 following hypotheses:

- 100 • The amount of available NSCs located in cambium or xylem sustains metabolic activity
101 of the living cells and influences the total number of cells produced
- 102 • Intrinsic (tissue preferentially supplying carbon) and extrinsic (water availability and
103 temperature) factors represent constraints to NSC availability and xylem production.

104

105

RESULTS

106 *Tree growth*

107 Radial growth of the irrigated saplings showed a typical S-shaped curve for all temperature
108 treatments (total cells, Figure 3). The increase in cell number was similar in non-irrigated and
109 irrigated saplings before the treatment. At the end of the water deficit, the increase in total cells
110 was observed to slow down or stop for several weeks in non-irrigated saplings, while growth
111 continued undisturbed in irrigated saplings. On DOY 200-220, a new sharp increase in radial
112 growth was observed in non-irrigated saplings, although the total cell number always remained
113 lower than in irrigated saplings until the end of the growing season.

114 In respect to radial growth (i.e. the increase in xylem cells), apical growth occurred quickly with
115 the maximum length being reached in 15-20 days (Figure 3). In both study years, this sharp
116 increase was synchronous between the different treatments and started when irrigation was
117 withheld. After the maximum apical length was reach, the observed deviations were caused by
118 sapling difference height growth, which was higher in 2011 compared with 2010.

119 Similar annual trends of living cells were observed between the temperature and water
120 treatments (Figure 3). The living cells were characterized by bell-shaped curves, with a
121 depression at about 1/3 of the growing season for both water and temperature treatments. In May
122 2010, cambium division and cell enlargement had already started, as indicated by a number of
123 cells varying between 10 and 20, depending on the temperature treatment (Figure 3). In May
124 2011 (around DOY 120), only the cambium was already active with 6–7 cells on average but no
125 cell differentiation. Around DOY 160-170, the number of living cells decreased to a minimum of
126 9-10 and 12-15 in 2010 and 2011, respectively. These drops in the living cell were synchronized
127 with the start of the apical growth of the saplings (Figure 3). After this drop, the number of living

128 cells increased rapidly to its maximum, while the increase was much slower in saplings subjected
129 to water deficit. Once annual activity had ended and the cambium stopped dividing, the number
130 of living cells gradually decreased to the minimum value, corresponding to quiescence
131 conditions of the cambium meristem. Between 4 and 6 cambial cells were observed in autumn,
132 fewer than at the beginning of the season (Figure 3).

133 *Correlations among NSCs*

134 In cambium of irrigated saplings, the variation of sucrose was mainly correlated with D-pinitol
135 ($r=0.53$), and marginally to raffinose ($r=0.30$) and fructose ($r=0.23$) (Table 1). Fructose varied
136 according to glucose with a correlation coefficient of 0.88. Fructose was marginally correlated
137 with D-pinitol ($r=0.31$). In xylem of irrigated samplings, the correlations between the soluble
138 sugars were slightly different. Sucrose was correlated with raffinose ($r=0.36$) but not with D-
139 pinitol (Table 1). The variation of D-Pinitol in the xylem was positively correlated with glucose
140 ($r=0.65$) and fructose (0.71) (Table 1). As for cambium, the variation of fructose and glucose in
141 xylem was highly similar ($r=0.98$).

142 In general, the correlations between the soluble sugars were mostly similar in saplings submitted
143 to water deficit. In cambium, sucrose was correlated with D-pinitol ($r=0.54$) and fructose
144 ($r=0.21$) but not with raffinose. However, D-pinitol and raffinose showed a positive correlation
145 ($r=0.23$). Sucrose was negatively correlated with fructose and glucose, as showed by the
146 correlation coefficients of -0.22 and -0.28 for, respectively.

147 *Variation in NSC*

148 NSCs measured in cambium or in xylem had similar trends irrespective of the treatments (Figure
149 4). Therefore, the means represent all temperature treatments confounded [see Deslauriers et al.

150 (2014) for full NSCs time series and statistical analyses]. In cambium, sucrose was up to 30
151 times more abundant than the other NSCs (Figure 4), followed by pinitol and fructose. In both
152 years, the withholding of irrigation caused a small decrease in sucrose and fructose and a sharp
153 increase in raffinose observed around the end of the water deficit period (Figure 4). Although the
154 concentrations of NSCs were much lower in the inner xylem, analogous trends to that of
155 cambium were observed in xylem.

156 Parallel variations were observed between NSCs and the number of living cells (Figure 3-4).
157 When cambial activity started, between DOY 120 and 130, the amount of NSCs in cambium was
158 high. A decline was observed between DOY 150 and 170, which was more pronounced in 2010
159 with concentrations close to zero. A second decline was observed in mid-July (DOY 208 in 2010
160 and DOY 196 in 2011).

161 **Mixed-effects model**

162 The results from the null models (total and living cells) showed that random effects were
163 significant, particularly at tree level with high ICC (Table 2). The random effects were therefore
164 included in the mixed-effects model. Random slopes and interactive effects of temperature \times
165 water treatments were not significant and so excluded from the final model. A full model was
166 built and considered the best model for the total xylem cells and living cells, respectively, in
167 terms of minimum AIC, AICC and BIC. Good performance of the two full models is also
168 reflected by their high conditional R^2 (over 0.79 for total cells and 0.49 for living cells).

169 We found that the increase in number of total xylem cells during the growing season can be
170 modeled as a function of sucrose, pinitol and water treatments, as well as random effects. For the
171 other model, the living cells can be modeled as a function of raffinose, sucrose, pinitol, fructose,
172 the tissue where the sugars were extracted, water and temperature treatments, as well as random

173 effects. Even if significant, fixed effects only accounted for a small portion of variance, as shown
174 by the lower PCV (Table 2) and marginal R^2 (Table 3). The majority of the variance was
175 explained by the random effects, as indicated by the lower PCV and large difference between the
176 marginal and conditional R^2 (Table 3). This could be explained by the high variance in the
177 measured cell numbers, especially for the total xylem cells (Figure 3). Nevertheless, the number
178 of total xylem cells and living cells changed positively or negatively according to the water
179 treatment and specific sugar compounds (Figure 5).

180 Both full models demonstrated that the water treatment was a significant variable to account for
181 the variations in cell number, particularly for the predicted total xylem cells ($P < 0.0001$, Table 2)
182 compared to living cells ($P < 0.05$, Table 2). In general, we found a decline in the variance of total
183 xylem cells and living cells explained under the water deficit treatment compared with the
184 irrigated treatment, as shown by the marginal R^2 when tissue and temperature were fixed (Table
185 3).

186 In terms of difference among temperature treatments, most of the temperature treatments were
187 not significant (Table 2). Therefore, temperature did not influence the variations in total xylem
188 cells and slightly explains the variation in the living cells ($P < 0.05$ for T+2 treatment only). The
189 variance of total xylem cells and living cells explained under the different thermal treatments
190 was generally higher in T0, T+6 Daytime and T+6 Nighttime compared to T+2 and T+5 as
191 shown by the marginal R^2 (Table 3). Compared with 2011, higher temperatures were registered
192 in 2010, mainly due to a warmer spring (Figure 2), with the greenhouse conditions being above
193 the long-term average calculated for the boreal stands.

194 The decomposition of variance (DOV) also precisely indicated the contribution of each fixed
195 effect to both dependent variables (Figure 6). The DOV indicated that water availability was a

196 crucial factor influencing the total number of xylem cells (73%), while sucrose (23%) and tissue
197 (23%) were both the most influent to predict the number of living cells. Of the NSCs
198 concentrations, pinitol (10.5%) and sucrose (7.9%) were significantly related to the total xylem
199 cells while all the carbon variables (sucrose, fructose, raffinose and pinitol, accounting for 59%
200 in total) were in turn significantly associated with the living cells (Figure 6). The tissue was
201 found to be a significant variable explaining the predicted living cells, as suggested by a higher
202 percentage of DOV. Interestingly, more variance in the predicted living cells can be accounted
203 for by the NSCs extracted from cambium than xylem, as indicated by higher marginal R^2 for
204 cambium under constant water and temperature treatments (Table 3). However, the variable
205 tissue was not significant for the predicted total xylem cells, as shown by a lower percentage of
206 DOV (0.14%) and more or less similar variance explained between cambium and xylem when
207 under the same water and temperature treatments (Table 2).

208 **Discussion**

209 In this study, xylogenesis was modeled as a function of NSCs availability and other intrinsic
210 (tissue) and extrinsic (water availability and temperature) factors. Similar variations between
211 xylogenesis and NSCs were also observed in conifers [larch and spruce (Simard et al., 2013)]
212 and broadleaves [poplar (Deslauriers et al., 2009)]. However, this is the first time that the
213 relationship has been mathematically quantified. We found that the NSCs measured in the
214 cambium zone were more important in explaining the variation in the number of living cells
215 during the growing season. This indicates the preference of mobile sugars probably coming from
216 the recently fixed carbon unloaded from phloem transport for the metabolic needs of growth. In
217 general, the variance explained in wood formation slightly decreases under water deficit
218 implying some uncoupling between NSCs and growth, while the warming had very few
219 significant effects.

220 **The role of available carbon during xylogenesis**

221 Given that wood formation was disentangled in total xylem and living cells, we were able to
222 elucidate the physiological mechanisms underlying the contribution of each NSCs variable and
223 water with both models (Figures 5-7). For living cells (all metabolically active), all the sugar
224 compounds were found to explain their variation with higher DOV for sucrose (22.66%) and
225 fructose (16.76%), followed by raffinose (13.19%) and pinitol (6.7%). The most important NSCs
226 explaining the total xylem cells were sucrose (7.88%) and pinitol (10.43%) only, as non-living
227 cells were included in the total xylem cells to account for the entire tree-ring development over
228 time (figure 7).

229 Sucrose was the main compound forming the NCS pool in cambium [see Figure 3 and
230 Deslauriers et al. (2014)]. This sugar is mainly broken down by invertase, forming hexose

231 (glucose and fructose), and by sucrose synthase, forming fructose and UDP-glucose (Koch,
232 2004). Large concentration gradients of sucrose and hexose can be observed between
233 meristematic (high sucrose) and differentiation zones (high hexose) in root tips (Scheible et al.,
234 1997; Freixes et al., 2002). Even though no spatial gradient of carbohydrate was measured in this
235 study, the amounts of both total xylem (meristematic activity) and living cells (metabolic
236 activity) were positively coupled with sucrose. Sucrose was the most important carbon
237 compound influencing the variability observed in living cells (Figure 5, middle panel) probably
238 because these were composed of a large number of tracheids undertaking secondary cell wall
239 formation (Deslauriers et al., 2014). Indeed, a large quantity of UDP-glucose is required during
240 the process of wall formation (CWT, Figure 1) as the number of cells in this phase represents an
241 irreversible sink for building the material composing the cell walls (cellulose, hemicellulose and
242 lignin), a process that lasts several weeks in conifers (Deslauriers et al., 2003; Gruber et al.,
243 2010; Cuny et al., 2014).

244 Moreover, the amount of living cells was explained by fructose (16.76%). As glucose was highly
245 correlated with fructose (correlation coefficient varying between 0.88 and 0.98), the contribution
246 and role of this sugar is expected to be similar to fructose. These results are in line with Freixes
247 et al. (2002) who found a positive correlation between root elongation and hexose concentration
248 in *Arabidopsis*. The hexose concentration is a good proxy for rapid expansion (Muller et al.,
249 2011). A large amount of hexose are produced from vacuolar invertase to increase cell osmotic
250 potential and generate the appropriate turgor pressure for cell expansion (Koch, 2004). Fructose
251 can also be used for ATP production (Koch, 2004) necessary for cell metabolism during the
252 growth processes or active transport of several compounds across membranes. The results for
253 fructose therefore support the fact that sugar allocation and partition could also be linked with

254 respiratory processes as the number of cambium and differentiating cells are related with CO₂
255 emitted by the stem during wood formation (Lavigne et al., 2004; Gruber et al., 2009).

256 The osmotically active sugars, D-pinitol and raffinose were also found significant. D-pinitol
257 explained both total xylem (DOV of 10.43) and living cells (DOV of 6.70) but with a negative
258 and positive influence, respectively (Figure 5, upper panel). Cyclitols, such as D-pinitol, are
259 normally implicated in cell osmoregulation in order to maintain cell turgor in the case of stress
260 [i.e. cold, drought or salinity, see review by Orthen et al. (1994)], which could explain the
261 negative influence of this sugar on the total xylem cell, especially under water deficit. However,
262 it cannot be excluded that D-pinitol might also contribute to the overall water potential
263 [maintaining turgor (Orthen et al., 1994; Johnson et al., 1996)] and explain the positive influence
264 on the living cells (Figure 5, lower panel). The growing cells first accumulated pinitol and
265 hexose in order to regulate cell osmosis to generate the turgor to enlarge and then shifted to more
266 complex sugars (i.e. raffinose) when the water potential drops (Deslauriers et al., 2014).

267 Raffinose drastically increases during water deficit because this sugar mainly acts as
268 osmoprotector and ROS scavenger (Nishizawa-Yokoi et al., 2008; dos Santos et al., 2011). The
269 negative effect of this sugar on the living cells (Figure 5, lower panel) is therefore perfectly in
270 line with its main role.

271 *The role of tissue in supplying NSCs*

272 Our mixed-effects model showed that NSCs extracted from cambium tissue were more important
273 as a source of NSCs to predict the amount of living cells (DOV of 22.61%), as shown by the
274 higher variance explained by cambium (Table 3). However, the variable tissue was not
275 significant in explaining the variation in total xylem cells possibly because non-living cells were
276 included to account for the tree-ring increase over the growing season. Compared with the

277 outermost xylem, much higher amounts of NSCs are found in cambium (Deslauriers et al., 2009;
278 Simard et al., 2013), because of its proximity to the unloading sites in phloem. The recently-
279 produced NSCs are thus preferred in terms of carbon allocation (Carbone et al., 2013; Steppe et
280 al., 2015) as phloem transport relies on the turgor pressure gradient created by the difference
281 between sugar loading and unloading processes (De Schepper et al., 2013), represented here by
282 the breakdown of sugars by the living cells (Figure 1 and 7). The bimodal pattern in the number
283 of living cells characterized by a slight depression in June is in agreement with previous
284 observations realized on conifer species (Rossi et al., 2009), which were supposed to be
285 associated with the internal competition for carbohydrates among meristems and the allocation
286 priority towards primary growth. This hypothesis is confirmed by reduction in sucrose measured
287 in cambium, especially in 2010, at the time of apical growth (DOY 160). In cambium, NSCs can
288 also come from the hydrolysis of maltose during the process of starch degradation in bark at the
289 beginning of the growing season (Oribe et al., 2003; Begum et al., 2013). Hence, our mixed-
290 model results are in line with CASSIA dynamic growth model results, suggesting that cambial
291 growth was sensitive to current-year carbon production (Schiestl-Aalto et al., 2015).

292 Girdling experiments – blocking down the phloem translocation of photosynthates – have also
293 demonstrated the foremost importance of current photoassimilate flux to sustain stem growth
294 (Daudet et al., 2005). While some girdling studies indicated that NSC reserves in the stem were
295 not sufficient to sustain growth below the girdle in the short or in the long term (de Schepper et
296 al., 2010; Maier et al., 2010), others demonstrated that stem reserves could be used to restart
297 growth (Daudet et al., 2005; Maunoury-Danger et al., 2010). This assumption imposes source –
298 sink relationships between xylem ray parenchyma cells and living cells (Olano et al., 2013). In
299 the stem, ray parenchyma cells are the connective tissues between the different compartments

300 (from the phloem to heartwood) and have many roles such as reserve storage (Gartner et al.,
301 2000) and respiration (Wolfgang, 1985; Spicer and Holbrook, 2007). This could explain why less
302 variance in the predicted living cells was represented by the NSCs extracted from the xylem
303 tissues, even during drought. C storage indeed has priority over growth, reflecting a safety
304 strategy in trees growing in cold or dry conditions. Hence, our result demonstrates that water is
305 much more limiting than inner soluble sugars, in agreement with Palacio et al. (2014).

306 *Effect of water deficit and warming*

307 The water deficit had a significant effect on both models, with a higher percentage of DOV on
308 total cells (73%) compared with living cells (15%). Fewer tracheids were produced at the end of
309 and after the period of water deficit. This was reflected first by the smaller populations of living
310 cells and second by a temporary plateau in the total number of cells (Figure 2). The mixed-model
311 results show that water availability was ranked as the most significant factor explaining total
312 xylem cell production, before any carbon factors (Figure 6). This modulation of growth under
313 low water is crucial to limit the number of living cells undertaking differentiation which need
314 water to fully complete their development. Otherwise, many differentiating cells would be
315 locked in enlargement, without enough water to generate the suitable wall-yielding turgor
316 pressure required for cell growth (Steppe et al., 2015). This key result confirms that radial
317 growth, expressed here as the number of cells produced, is not source-limited (Körner, 2003;
318 Rocha, 2013; Palacio et al., 2014) because cambium is inhibited at a lower level of water stress
319 than photosynthesis (Muller et al., 2011; Balducci et al., 2013; Fatichi et al., 2014). Similar
320 conclusions were obtained with CASSIA dynamic growth model (Schiestl-Aalto et al., 2015).
321 For the living cells however, water availability was ranked in fifth position after carbon (sucrose,
322 fructose, raffinose) and tissue (cambium). The apparent contradiction between these results could

323 be explained by the low number of cambial cells with respect to differentiating cells, especially
324 wall-thickening cells, and by the sugar compounds needed to build and maintain the turgor
325 pressure of enlarging cells (Pantin et al., 2013; Steppe et al., 2015). In other words, once
326 temperature and water availability are sufficient for cambial cells to divide, sugar compounds are
327 allocated to start expansion (i.e. attracting water molecules) and afterwards, to thickening the cell
328 walls.

329 The variance explained in both total xylem and living cells (as shown by the marginal R^2 when
330 tissue and temperature treatment were fixed) decreased under water deficit, showing some
331 uncoupling between NSCs and growth, especially for the living cells. This reduction could
332 represent an alteration of NSCs dependence on growth, caused by the reduced water availability
333 (Muller et al., 2011): (1) Because wood formation practically stopped during water deficit, NSCs
334 could be less required for wood formation processes (i.e. sink-limitation), which in turn, could
335 reduce the variance explained; (2) In response to water deficit, the flow of available carbon,
336 especially in the form of sucrose, could be further directed to osmoregulation (i.e. forming
337 raffinose) at the expense of growth. Although the quantities are minor, these carbohydrates are
338 unavailable for osmotic purposes when sequestered in cell structures (cell wall and vacuoles)
339 (Pantin et al., 2013); (3) The accessibility and utilization of NSCs during water deficit is
340 questioned (Sevanto et al., 2014) because the movement of NSCs decreases under low water
341 content (Woodruff and Meinzer, 2011) and translocation of carbohydrates in phloem becomes
342 more limited under water stress (Woodruff, 2014).

343 The contribution of temperature in explaining total xylem cells was non-significant while only
344 T+2 was significant in explaining the number of living cells (2.63%), showing a marginal effect
345 of temperature in our experiment. Although temperature is important in determining the potential

346 growth rate (Pantin et al., 2012), little difference was found in wood formation (Balducci et al.,
347 2013) possibly because the onset of growth was similar between treatments and the temperatures
348 were well above the threshold limit for growth (Rossi et al., 2008) due to the greenhouse
349 conditions. Lower amount of hexose (Deslauriers et al., 2014) and starch in the ray parenchyma
350 cells (Balducci et al., 2013) was measured under warmer growth temperature, confirming the
351 results of Way and Sage (2008) in black spruce trees. Although acclimation occurs, the increase
352 in respiratory rate at higher temperature (Atkin and Tjoelker, 2003; Turnbull et al., 2004), may
353 reduce the hexose pool in cambium and xylem. Even if this suggests a lower carbon availability
354 for growth (particularly for cell enlargement), more studies are needed to characterize the role of
355 temperature, especially under natural conditions.

356 **Conclusion**

357 Our analyses provide, for the first time, quantitative relationships linking NSCs and xylem
358 development and including the influence of the nearby supply of carbon, water availability and
359 temperature. The mixed-model elaborated in this study confirmed earlier observations about the
360 parallel variation of sugars and differentiating xylem cells and is in line with the dynamic growth
361 model. These results have important implications at large ecological scale because cambial
362 activity is responsible for the permanent sequestration of carbon in the woody tissues (Cuny et
363 al., 2015). The understanding of how carbon and water availability influence secondary growth is
364 fundamental to improve growth models (Fatichi et al., 2014) and, in this sense, we provide
365 empirical knowledge on important C compartments, xylem and cambium, and their respective
366 roles in structural growth, including meristematic activity and tissues formation. However, our
367 investigation was based on black spruce sapling, which might have different dynamics of carbon
368 requirements and allocation compared to older trees, or trees of other species, especially if

369 deciduous. Despite the mechanisms of xylem growth remain the same across ontogenetic states
370 and species, caution in generalization of the results of this study for all trees must be taken due to
371 the potential variations in the timings and rates of carbon source (photosynthesis) and sinks
372 (wood formation).

373

METHODS

374

375 **Experimental design**

376 The experiment was performed in a greenhouse complex located in Chicoutimi (QC), Canada
377 (48° 25' N, 71° 04' W, 150 m above sea level) equipped with an automatic warming and cooling
378 system that controls the environmental parameters. Four-year-old black spruces [*Picea mariana*
379 (Mill.) B.S.P.]) were transplanted into 4.5 l plastic pots with a peat moss, perlite and vermiculite
380 mix, and left in an open field during a growing season and the following winter. In April 2010
381 and 2011, the saplings were taken into three different sections of the greenhouse for the
382 experiment and fertilized with 1 g l⁻¹ of NPK (20-20-20) dissolved in 500 ml of water (Balducci
383 et al., 2013). Three hundred saplings were installed in every section in both years, with a buffer
384 zone of one additional row of saplings at the borders. Saplings were 48.9 ± 4.7 cm tall with a
385 diameter of 8.0 ± 2.0 mm at the root collar, and were provided with drip trickles for irrigation.

386 In one section of the greenhouse, the temperature was set to mimic the current thermal condition
387 of the region (T+0). It was therefore maintained as close as possible to the external air
388 temperature, except on days of the year (DOY) 142 – 152 in 2010, when a technical problem
389 occurred. The two other sections were subjected to specific thermal regimes (Figure 2). In 2010,
390 the treatments (called T+2 and T+5) consisted of a temperature 2 and 5 K higher than T+0,
391 respectively (Balducci et al., 2013). In 2011, the treatments (called T+6 Daytime and T+6
392 Nighttime) were 6 K warmer than T0 during the day (T+6 Daytime, from 07:00 to 19:00) or
393 during the night (T+6 Nighttime, from 19:00 to 07:00) (Figure 2).

394 Two irrigation treatments were applied: (1) irrigated, consisting of maintaining the soil water
395 content at approximately 80% of field capacity; (2) water deficit, in which irrigation was
396 withheld from mid-May to mid-June, the period when cambium is vigorously dividing (Rossi et

397 al., 2006). At the end of the water deficit period, the soil water content of non-irrigated saplings
398 was less than 10%, while that of irrigated saplings varied between 40 and 50%. The predawn leaf
399 water potential (Ψ_{pd}) of irrigated saplings was maintained close to -0.5 MPa in both years.
400 During the water deficit, Ψ_{pd} of non-irrigated saplings dropped in response to the decrease of soil
401 water availability, reaching the lowest values on DOY 172 (-2.7 ± 0.2 MPa) and DOY 180 ($-$
402 1.3 ± 0.7 MPa) in 2010 and 2011, respectively. One week after the resumption of irrigation, Ψ_{pd} of
403 irrigated and non-irrigated saplings were similar, showing that the saplings were able to recover
404 an optimal water status after the stress (Balducci et al., 2013; Deslauriers et al., 2014).

405 **Xylem growth**

406 From May to September 2010 and 2011, stem disks were collected weekly at 2 cm from the root
407 collar of 36 randomly-selected saplings (6 saplings \times 2 water regimes \times 3 thermal treatments). At
408 the same time, the apical growth (mm) was measured on each sapling with a precision digital
409 calibre to the nearest 1 mm. The collected stem disk were dehydrated with successive immersions
410 in ethanol and D-limonene, embedded in paraffin and transverse sections of 8-10 μ m thickness
411 were cut with a rotary microtome (Rossi et al., 2006).

412 The sections were stained with cresyl violet acetate (0.16% in water) and examined within 10-25
413 minutes with visible and polarized light at magnifications of 400-500 \times to distinguish the
414 developing xylem cells. For each section, (i) cambial, (ii) enlarging, (iii) cell-wall thickening and
415 (iv) mature cells were counted along three radial files. In cross section, cambial cells were
416 characterized by thin cell walls and small radial diameters. During cell enlargement, the
417 tracheids still showed thin primary walls but radial diameters were at least twice those of the
418 cambial cells. Observations under polarized light discriminated between enlarging and cell wall

419 thickening tracheids. Because of the arrangement of the cellulose microfibrils, the developing
420 secondary walls glistened when observed under polarized light, whereas no glistening was
421 observed in enlargement zones where the cells were still just composed of primary wall
422 (Deslauriers et al., 2003). The progress of cell wall lignification was detected with cresyl violet
423 acetate that reacts with the lignin (Rossi et al., 2006). Lignification appeared as a colour change
424 from violet to blue. A homogeneous blue colour over the whole cell wall revealed the end of
425 lignification and the reaching of tracheid maturity (Gričar et al., 2005).

426 **NSC extraction and assessment**

427 Every two weeks, 18 of the 36 saplings used for xylem analysis were selected for NSCs
428 assessment (3 saplings × 2 water regimes × 3 thermal treatments). The branches were removed
429 and the bark separated from the wood to expose the cambial zone of the stem. The two parts
430 (bark and wood) were plunged into liquid nitrogen and stored at -20 °C. Dehydration was
431 performed with a 5-days lyophilisation. The cambium zone, probably including some cells in
432 enlargement, was manually separated by scraping the inner part of the bark and the outermost
433 part of xylem with a surgical scalpel (Giovannelli et al., 2011). After having removed the
434 cambium, the wood was milled to obtain a fine powder.

435 Soluble carbohydrates extraction followed the protocol of Giovannelli et al. (2011). For the
436 cambium, only 1-30 mg of powder was available and used for the sugar extraction, while 30-600
437 mg of powder was available for wood. Samples with less than 1 mg of cambium powder were
438 not considered, this quantity being lower than the HPLC detection limit. Soluble carbohydrates
439 were extracted three times at room temperature with 5 ml of ethanol 75% added to the powder. A
440 100 µl volume of sorbitol solution (0.01g/ml) was also added at the first extraction as an internal
441 standard. In each extraction, the homogenates were gently vortexed for 30 minutes and

442 centrifuged at 10,000 rpm for 8 minutes. The three resulting supernatants were evaporated and
443 recuperated with 12 ml of nano-filtered water. This solution was then filtered by the solid phase
444 extraction (SPE) method using a suction chamber with one column of *N+* *quaternary amino*
445 (200 mg/3ml) and one of *CH* (200mg/3ml). The solution was evaporated until 1.5 ml and filtered
446 through a 0.45 μ m syringe filter into a 2 ml amber vial.

447 An Agilent 1200 series HPLC with a RID and a Shodex SC 1011 column and guard column,
448 equipped by an Agilent Chemstation for LC systems program, was used for soluble
449 carbohydrates assessment. Calculations were made following the internal standard method
450 described in Harris (1997). A calibration curve was created for each carbohydrate using pure
451 sucrose, raffinose, glucose, fructose (Canadian Life Science) and D-pinitol (Sigma-Aldrich). All
452 fitting curves had R^2 of 0.99 and F-values close to one, indicating that each sugar had a 1:1 ratio
453 with sorbitol. The quantity of sugar loss during extraction was calculated by comparing the
454 concentrations of sorbitol added at the beginning of the extraction to those of unmanipulated
455 sorbitol. The loss percentages were then calculated and added to the final results (Deslauriers et
456 al., 2014).

457 **Statistical analysis**

458 A mixed-effects model was used to fit the hierarchical data, in which an autocorrelation error
459 structure in the repeated measurements over time was extended to Level 1 [AR(1)] that was
460 nested within the measurements of different NSC concentrations (Level 2) extracted from
461 different tissues (Level 3, figure 1) of the randomly selected trees (Level 4). The trees were
462 nested under different temperature treatments (Level 5) and water treatments (Level 6). In
463 addition, there was a nested error structure, i.e., correlation among trees within temperature and
464 water treatments. The mixed-effects model can effectively deal with this nested error structure to

465 account for correlation associated with clustered data. Mixed-effects model techniques estimate
 466 fixed and random parameters simultaneously and give unbiased and efficient estimates of fixed
 467 parameters (Pinheiro and Bates, 2000).

468 Prior to the modeling analysis, the normality was checked and square root of data transformation
 469 was then applied to the number of living cells and total xylem cells to meet the assumption of
 470 normality. Note that hereinafter the transformed data were used in the mixed-effects model
 471 analysis. Variance inflation factors [VIF, Belsley et al. (1980)] were also calculated to detect
 472 multicollinearity among the predictors including sucrose, pinitol, glucose, fructose and raffinose.
 473 VIFs were generally lower than the accepted value of 4 (O'Brien, 2007) except for fructose that
 474 had a VIF > 10 due to collinearity with glucose, so was then removed from the model. Fructose
 475 was kept as this sugar is the product of both sucrose synthase and invertase.

476 Fixed effects included different NSC concentrations (raffinose, sucrose, pinitol, fructose),
 477 measured tissue (xylem and cambium), temperatures (control T+0, versus T+2, T+5, T+6
 478 Daytime and T+6 Nighttime) and water availability (water deficit and irrigated), and the
 479 interaction temperature × water. Random effects included trees and repeated measurements over
 480 time. In order to verify the two hypotheses, a mixed-effects model was built starting from a null
 481 model and then gradually extended to the higher levels (Singer, 1998). Therefore a mathematical
 482 function can theoretically be expressed by both fixed and random effects as follows:

$$483 \quad Y_{i(jklmt)} = \beta_0 + (\beta_1 + \mu_{1k})R_{i(jklmt)} + (\beta_2 + \mu_{2k})S_{i(jklmt)} + (\beta_3 + \mu_{3k})P_{i(jklmt)} + (\beta_4 + \mu_{4k})F_{i(jklmt)} + \beta_5 O_{jklm} + \beta_6 T_{lm} + \beta_7 W_m + \beta_8 T_{l(m)}W_m + \mu_{0k} + \varepsilon_{i(jklmt)}$$

484

485 where,

486 $Y_{i(jklmt)}$ is the *ith* ($i=1$ to 3) measured cell number from the *jth* tissue ($j= 0$ and 1, indicating
 487 xylem and cambium, respectively) in the *kth* tree ($k=1$ to 12) under the *lth* temperature

488 treatment ($l=0$ to 4, indicating T+0, versus T+2, T+5, T+6 Daytime, and T+6 Nighttime,
 489 respectively) and the m th water availability ($m=0$ and 1, indicating water deficit and
 490 irrigated, respectively) on day t ;

491 β_0 is the overall mean; β_1, β_2, \dots and β_8 are the corresponding fitted parameters;

492 $R_{i(jklmt)}, S_{i(jklmt)}, P_{i(jklmt)},$ and $F_{i(jklmt)}$ is the i th measured NSC concentrations (raffinose,
 493 sucrose, pinitol, and fructose, respectively) from the j th tissue in the k th tree under the l th
 494 temperature treatment and the m th water treatments on day t .

495 $T_{l(m)} \times W_m$ is the temperature*water interactive effects;

496 μ_0 is random intercept, and μ_1, μ_2, μ_3 and μ_4 are random slopes,

497 where
$$\begin{pmatrix} \mu_0 \\ \mu_1 \\ \mu_2 \\ \mu_3 \\ \mu_4 \end{pmatrix} \sim N \left[\begin{pmatrix} 0 \\ 0 \end{pmatrix}, \begin{pmatrix} \tau_{00} & \tau_{01} \\ \tau_{10} & \tau_{11} \end{pmatrix} \right], \tau_{00} \text{ and } \tau_{11} \text{ are the elements representing the variance}$$

498 components for the intercept and slope, respectively; τ_{10} is the covariance component
 499 representing correlation between the intercept and slope.

500 $\varepsilon_{i(jklmt)}$ is the random error associated with the i th measurements from the j th tissue of the
 501 k th tree under the l th temperature treatment and the m th water treatments on day t , $\varepsilon_{i(jklmt)}$
 502 $\sim N(0, \sigma_\varepsilon^2 \Omega)$, where

503
$$\sigma_\varepsilon^2 \Omega = \frac{\sigma_\varepsilon^2}{(1-\rho^2)} \begin{bmatrix} 1 & \rho & \rho^2 & \dots & \rho^{n-1} \\ \rho & 1 & \rho & \dots & \rho^{n-2} \\ \rho^2 & \rho & 1 & \dots & \rho^{n-3} \\ \cdot & \cdot & \cdot & \dots & \cdot \\ \rho^{n-1} & \rho^{n-2} & \rho^{n-3} & \dots & 1 \end{bmatrix}, \rho \text{ is the autocorrelation coefficient, } |\rho| < 1.$$

504 The mixed-effects model was built according to the conventional building process (Singer,
 505 1998); the detailed mathematical or statistical approaches used can be found in (Huang et al.,
 506 2014). A marginal R^2 , which was calculated on the fixed effects only, and a conditional R^2 ,
 507 which was calculated on both fixed and random effects (Nakagawa and Schielzeth, 2013) were
 508 also provided to assess the overall performance of a mixed-effects model.

509 [a]
$$R_{marginal}^2 = \frac{\delta_f^2}{\delta_f^2 + \delta_{tree}^2 + \delta_{ar(1)}^2 + \delta_\epsilon^2 + 0.25}$$

510 [b]
$$R_{conditional}^2 = \frac{\delta_f^2 + \delta_{tree}^2 + \delta_{ar(1)}^2}{\delta_f^2 + \delta_{tree}^2 + \delta_{ar(1)}^2 + \delta_\epsilon^2 + 0.25}$$

511 Where, δ_f^2 is the variance calculated from the fixed effect components of the mixed model and
 512 was estimated through multiplying the design matrix of the fitted effects with the vector of fixed
 513 effects estimates, i.e., predicting fitted values based on fixed effects alone, followed by
 514 calculating the variance of these fitted values; δ_{tree}^2 is the variance at tree level; $\delta_{ar(1)}^2$ is the
 515 variance for the first order autocorrelation term; δ_ϵ^2 is the variance for the error term; 0.25 is the
 516 distribution-specific variance linked by square root.

517 To provide information regarding the variance explained at each level, the proportion change in
 518 variance (PCV) was calculated according to (Merlo et al., 2005):

519 [c]
$$PCV_{tree} = 1 - \frac{\delta_{tree}^2}{\delta_{tree(null)}^2}$$

520 [d]
$$PCV_{ar(1)} = 1 - \frac{\delta_{ar(1)}^2}{\delta_{ar(1)(null)}^2}$$

521 [e]
$$PCV_{residual} = 1 - \frac{\delta_{residual}^2}{\delta_{residual(null)}^2}$$

522 Where, $\delta^2_{tree(null)}$, $\delta^2_{ar(1)(null)}$ and $\delta^2_{residual(null)}$ is the variance from the null model, respectively;

523 δ^2_{tree} , $\delta^2_{ar(1)}$ and $\delta^2_{residual}$ is the variance from the full model, respectively.

524 The assumption of normality of the residuals was also verified. In addition, the decomposition of
525 variance (*DOV*) (Huang et al., 2013; Huang et al., 2014) was performed to further quantify how
526 much variance in the predicted square root of total xylem and living cells can be attributed to
527 different fixed-effects predictors using SAS Proc GLM (type III). All analyses were conducted
528 with SAS (Version 9.3, SAS Institute Inc. Carry, NC, USA).

529

530 **Acknowledgements**

531 The authors thank J. Allaire, D. Gagnon and C. Soucy for technical support and A. Garside for
532 checking the English text.

533 **List of authors contributions**

534 AD and SR elaborate the concept behind the experiment, AD wrote the text helped by all the
535 other authors, JGH elaborate and realized the mixed model effect, MB and LB made the
536 sampling and the NSCs and wood formation analysis respectively.

537 **Table 1.** Pearson correlation coefficients between NSCs. In irrigated sampling (left part), the correlations were performed between the
 538 soluble sugars measured in cambium (grey background, n=188) and xylem (white background, n=223). In water deficit sampling
 539 (right part), the correlations were performed between the soluble sugars measured in cambium (grey background, n=163) and xylem
 540 (white background, n=215). Asterisks indicate significant correlation coefficients P<0.0001 (***); P<0.001 (**); P<0.05 (*). Suc –
 541 sucrose; Pin – pinitol; Fru – fructose; Glu – glucose; Raf – raffinose.

542

	Irrigated					Water deficit				
	Suc	Pin	Fru	Glu	Raf	Suc	Pin	Fru	Glu	Raf
Suc	–	0.53***	0.23*	0.02	0.30***	–	0.54***	0.21*	0.04	0.08
Pin	0.20**	–	0.31***	0.05	0.08	0.15*	–	0.28**	0.12	0.23*
Fru	-0.08	0.71***	–	0.88***	0.28***	-0.22**	0.57***	–	0.89***	0.08
Glu	-0.15*	0.65***	0.98***	–	0.17*	-0.28***	0.46***	0.97***	–	0.00
Raf	0.36***	0.09	0.25***	0.26***	–	0.27***	0.09	0.04	0.02	–

543

544 **Table 2.** Statistics of the null and full models built for the predicted total xylem (left) cells and living cells (right). Standard error (SE)
 545 is reported in parentheses; P<0.0001 (***); P<0.001 (**); P<0.05 (*); ICC, Intra-class correlation; PCV, Proportion change in
 546 variance.

Dependent variables Model <i>n</i>	Total xylem cells		Living cells	
	Null model ($\times 10^{-2}$) 6357	Full model ($\times 10^{-2}$) 6264	Null model ($\times 10^{-2}$) 6360	Full model ($\times 10^{-2}$) 6267
Fixed effects				
Intercept (β_0)	591.61 (8.74)***	620.00 (28.18)***	368.17 (1.90)***	331.43 (7.50)***
Raffinose (β_1)		-0.21 (1.42)		-1.45 (0.43)***
Sucrose (β_2)		0.47 (0.20)*		0.27 (0.06)***
Pinitol (β_3)		-1.85 (0.51)***		0.51 (0.19)**
Fructose (β_4)		-0.02 (1.13)		1.35 (0.36)***
Tissue (xylem, β_5 versus cambium)		6.52 (23.86)		28.27(6.42)***
Temperature (<i>warm versus T+0</i>)				
Temperature (T+2) (β_6)		45.86 (25.78)		12.02 (5.40)*
Temperature (T+5) (β_6)		34.79 (25.72)		7.20 (5.42)
Temperature (T+6 daytime) (β_6)		-11.04 (25.70)		1.82 (5.44)
Temperature (T+6 nighttime) (β_6)		-24.03 (25.66)		-0.34 (5.46)
Water (water deficit, β_7 versus irrigated)		-70.26 (17.06)***		-11.06 (3.62)*
Random effects				
Residuals (additive dispersion)	111.81 (2.41)***	108.98 (2.37)***	24.11 (0.60)***	23.94 (0.59)***
Tree (tissue \times temperature \times water)	528.91 (29.18)***	493.02 (27.66)***	20.42 (1.44)***	17.57 (1.28)***
Repeated measurement (tree) [AR(1)]	21.63 (1.48)***	21.18 (1.50)***	31.53 (1.58)***	30.69 (1.58)***
ICC (measurements)	3.27 %		41.45%	
ICC (tree)	79.85 %		26.85%	
PCV (measurements)		2.08%		2.66%
PCV (tree)		6.79%		13.96%
PCV (residuals)		2.53%		0.71%
Model fit				
-2 Log Likelihood	20871.7	20395.4	9556.1	9335.1
AIC	20879.7	20423.4	9564.1	9363.1
AICC	20879.7	20423.4	9564.1	9363.2
BIC	20871.7	20395.4	9556.1	9335.1

547

548 **Table 3.** The marginal and conditional R² (%) explained by the full model for total xylem cells
 549 and living cells under different treatments. The treatments are expressed as the combination of
 550 tissue (xylem *versus* cambium), water treatment (irrigated *versus* water deficit) and temperature
 551 treatment (T+0 *versus* T+2, T+5, T+6 Daytime and T+6 Nighttime)

552

Treatment combinations	Total xylem cells		Living cells	
	Marginal R ²	Conditional R ²	Marginal R ²	Conditional R ²
<i>Cambium – Irrigated</i>				
T+0	1.20	79.58	4.79	52.06
T+2	0.27	79.39	2.66	50.99
T+5	2.07	79.76	2.91	51.11
T+6 Daytime	1.02	79.54	3.63	51.48
T+6 Nighttime	1.55	79.65	4.79	52.06
<i>Cambium – Water deficit</i>				
T+0	0.82	79.50	4.34	51.83
T+2	2.81	79.91	2.57	50.94
T+5	0.84	79.50	2.62	50.97
T+6 Daytime	0.94	79.52	4.06	51.69
T+6 Nighttime	0.68	79.47	4.34	51.83
<i>Xylem – Irrigated</i>				
T+0	1.10	79.56	0.85	50.08
T+2	0.25	79.38	0.20	49.75
T+5	0.44	79.42	0.19	49.75
T+6 Daytime	0.17	79.37	0.06	49.68
T+6 Nighttime	1.01	79.54	0.85	50.08
<i>Xylem – Water deficit</i>				
T+0	0.03	79.34	0.48	49.90
T+2	0.43	79.42	0.06	49.68
T+5	0.03	79.34	0.10	49.70
T+6 Daytime	0.61	79.46	0.05	49.68
T+6 Nighttime	0.44	79.42	0.48	49.89

553

554

555 **Figure legends**

556 **Figure 1.** Differentiating cells during wood formation (C, cambium; ENL, enlargement; CWT,
557 cell wall thickening) and the mature cell (M). The living cells in the analyses included C, ENL
558 and CWT while the total cell represents ENL, CWT and M cells. The available NSCs were
559 measured in the cambium and xylem. PH; living phloem.

560 **Figure 2.** Temperature measured during the experiments in 2010 (left) and 2011 (right). In 2010
561 the temperature treatments were T+0 (blue line), T+2 (red line) and T+5 (black line). In 2011,
562 the temperature treatments were T+0 (blue line), T+6 Daytime (red line) and T+6 Nighttime
563 (black line). The grey bands represent the period when irrigation was withheld during both years.

564 **Figure 3.** Dynamics of wood formation in 2010 (left) and 2011 (right) represented as the mean.
565 The living cell represents the sum of cambial cells, cells in enlargement and in wall formation.
566 The total cell represents tree ring growth as the sum of cells in enlargement, in wall formation
567 and mature cell. In 2010 the temperature treatments were T+0 (blue line), T+2 (red line) and T+5
568 (black line). In 2011, the temperature treatments were T+0 (blue line), T+6 Daytime (red line)
569 and T+6 Nighttime (black line). The grey background indicates the period when irrigation was
570 withheld. SD; standard deviation among the measured values in the corresponding graph.

571 **Figure 4.** Mean soluble sugars in cambium and xylem measured during 2010 and 2011. The
572 vertical bars represent the standard deviation among the measured trees (all temperature
573 treatments confounded). Open circles represent the irrigated plants, and filled circles water
574 deficit plants. The grey bands indicate the period when irrigation was withheld. Note the
575 different ranges of the vertical axes between cambium and xylem.

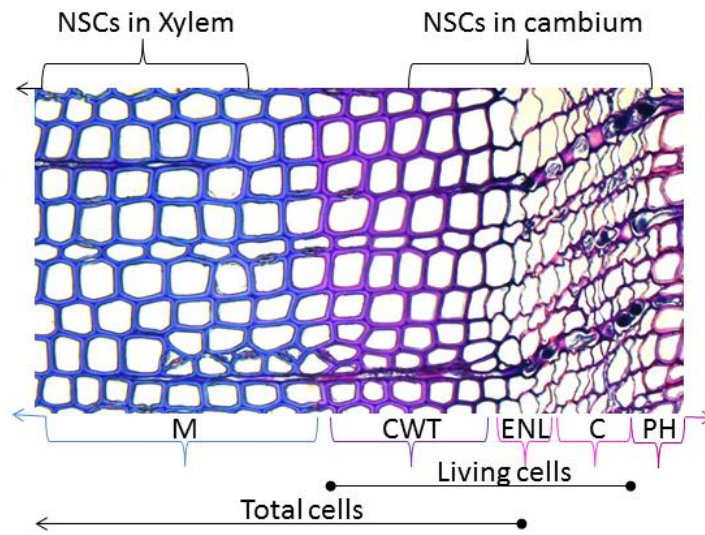
576 **Figure 5.** Surface plot (after smoothed spline interpolation based on n=3348 for irrigated and
577 n=2937 for water deficit). The relationships are illustrated between the predicted total xylem
578 cells (square root) and sucrose and pinitol (upper panel), and between the predicted living cells
579 (square root) and sucrose and fructose (middle panel), and raffinose and pinitol (lower panel).
580 The unit for sucrose, pinitol, fructose, raffinose is mg g⁻¹ dry weight (mg g⁻¹ d wt).

581 **Figure 6.** Mixed model decomposition of variance (DOV, percentage %) in predicting total
582 xylem cells (dark green) and living cells (light green).

583 **Figure 7.** Illustration of the observed wood formation processes expressed as the total xylem
584 cells (upper panel) and living cells (lower panel) in the presence (red) and absence (blue) of
585 water deficit (horizontal grey bars). Illustration of wood formation at the beginning of wood
586 formation is shown to illustrate the measured processes. The implications of the DOV's result
587 are explained to stress the contribution of the factors in wood formation (see discussion for full
588 explanation).

589

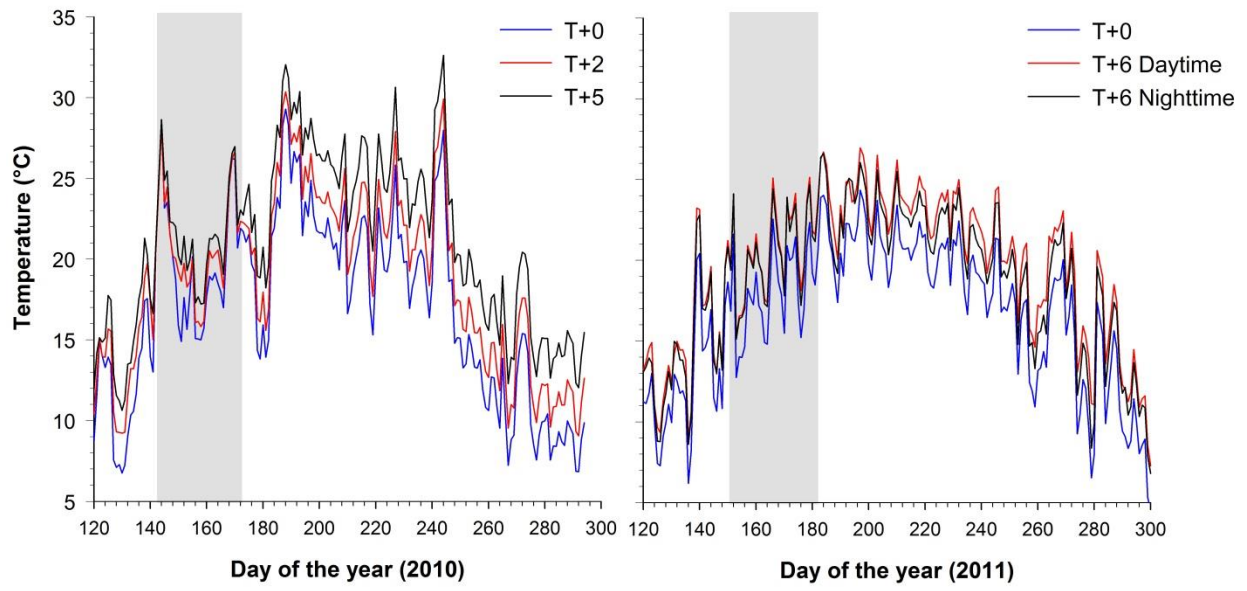
591 Figure 1



592

593

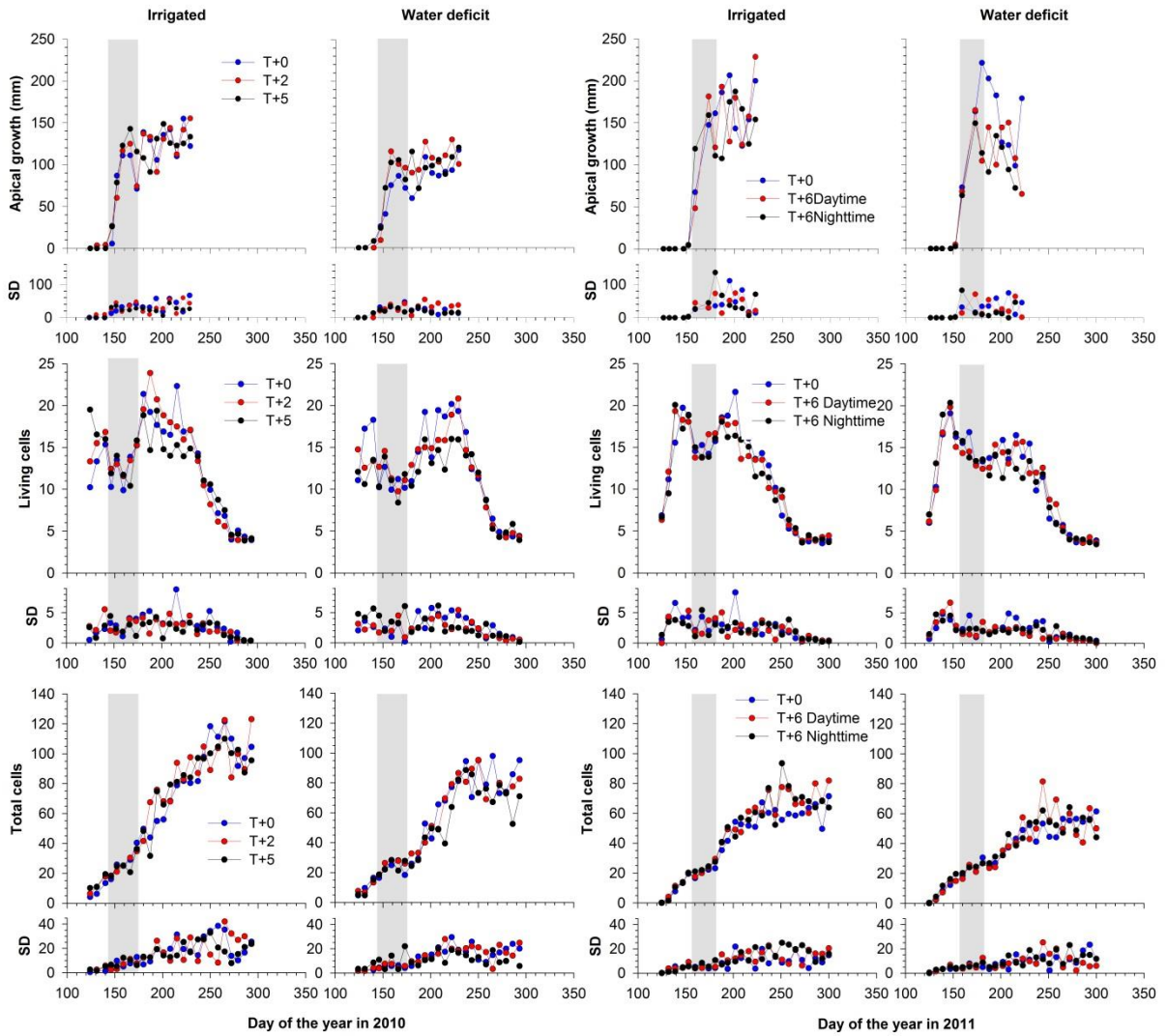
594 Figure 2



595

596

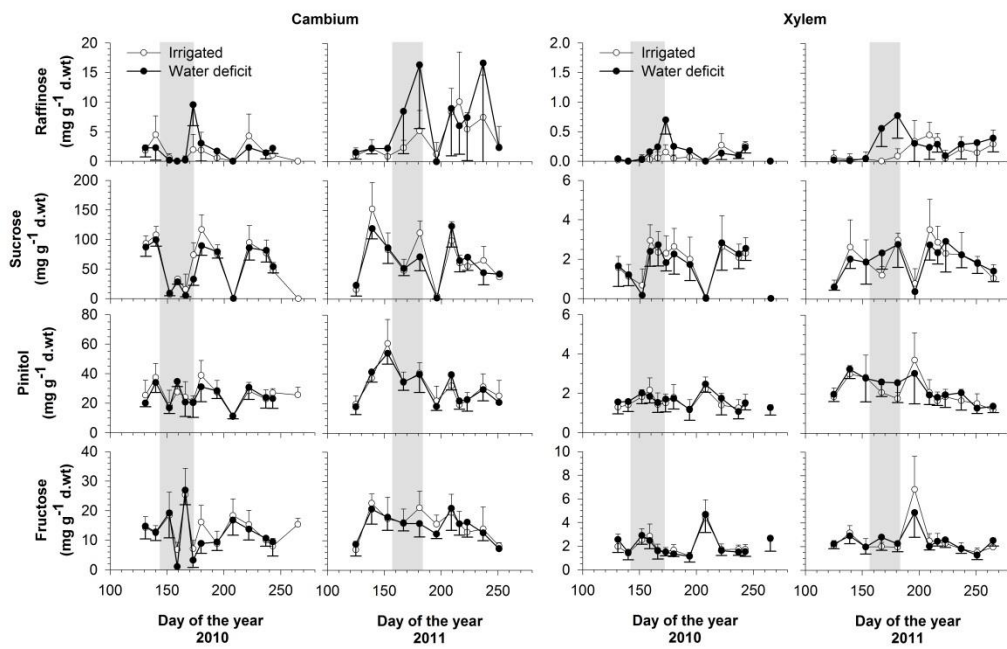
597 Figure 3



598

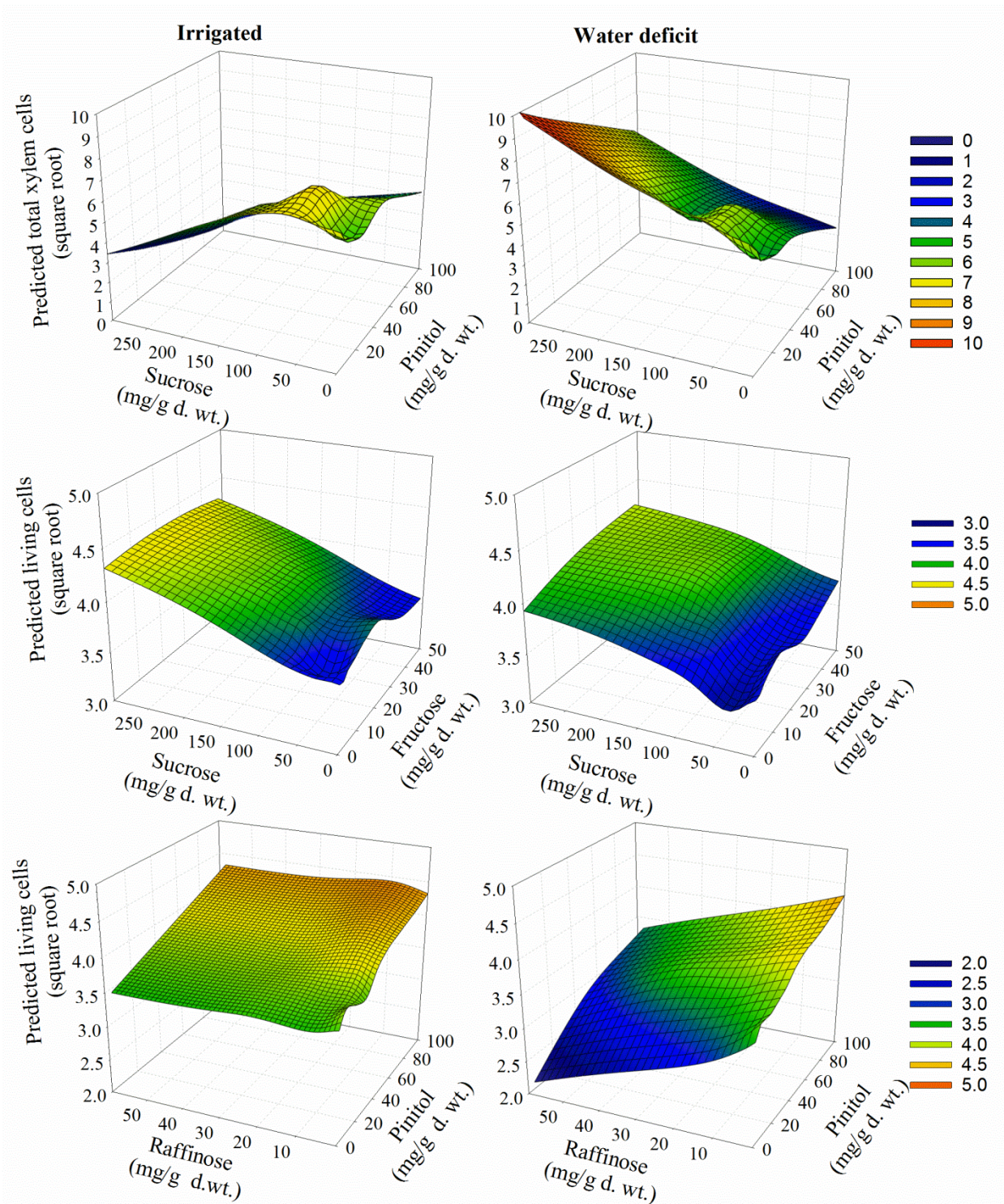
599

600 Figure 4



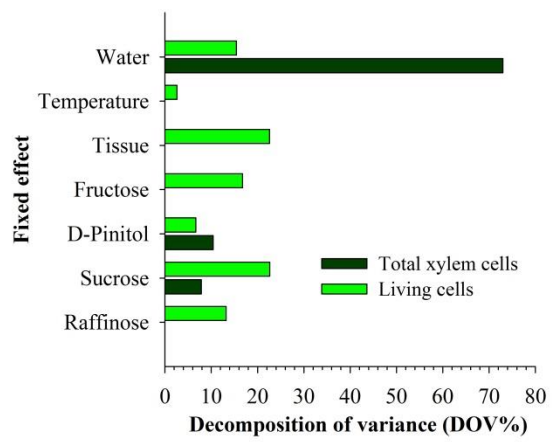
601

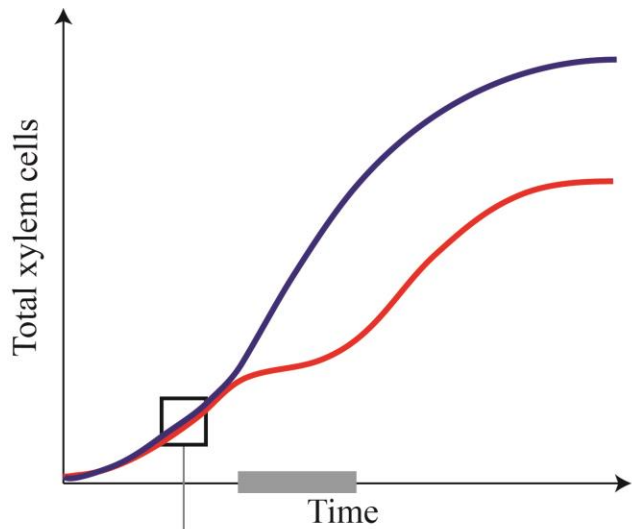
602



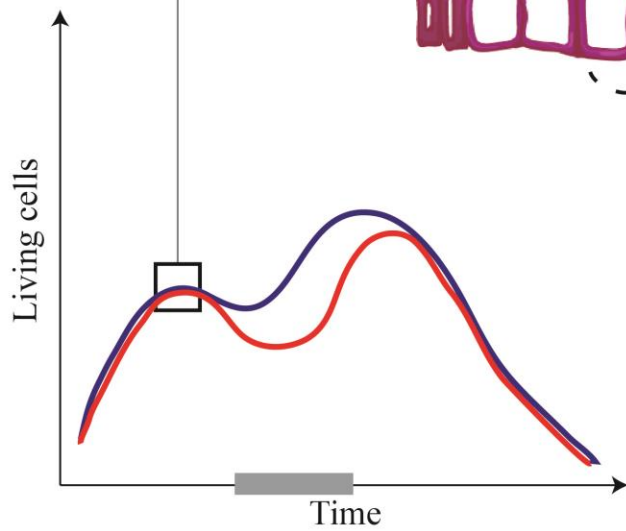
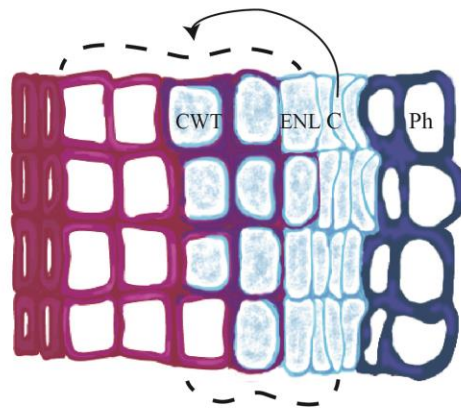
604

605





Meristematic activity
Water (73%) considered as first constraint in modulating the production of xylem from the cambial cells (C) during the growing season. Cambium (C) stops dividing in case of water deficit to limit the number of cells locked in differentiation without enough water. **Carbon** (18% in total) come as a second constraint with a negative effect of pinitol and a positive effect of sucrose.



Building stage
Carbon (59% in total) was the main factor modulating the number of living cells. The forms of sucrose and fructose were the most important, acting either indirectly to attract water molecules for building the required turgor pressure for cell enlargement (ENL) or directly, for building the cell wall (CWT). The carbon is preferentially coming from the **nearby cambium** (23%). **Water** (15%) operates as a subsequent limiting factor in building turgor pressure.

610 **References**

- 611 **Atkin OK, Tjoelker MG** (2003) Thermal acclimation and the dynamic response of plant respiration to
612 temperature. *Trends in Plant Science* **8**: 343–351
- 613 **Balducci L, Deslauriers A, Giovannelli A, Rossi S, Rathgeber CBK** (2013) Effects of temperature and
614 water deficit on cambial activity and woody ring features in *Picea mariana* saplings. *Tree*
615 *Physiology* **33**: 1006-1017
- 616 **Begum S, Nakaba S, Yamagishi Y, Oribe Y, Funada R** (2013) Regulation of cambial activity in relation to
617 environmental conditions: Understanding the role of temperature in wood formation of trees.
618 *Physiologia Plantarum* **147**: 46-54
- 619 **Belsley D, Kuh E, Welsch R** (1980) Regression diagnostics: Identifying influential data and sources of
620 collinearity. John Wiley & Sons, New York, USA
- 621 **Carbone MS, Czimczik CI, Keenan TF, Murakami PF, Pederson N, Schaberg PG, Xu X, Richardson AD**
622 (2013) Age, allocation and availability of nonstructural carbon in mature red maple trees. *New*
623 *Phytol* **200**: 1145-1155
- 624 **Cuny HE, Rathgeber CBK, Frank D, Fonti P, Fournier M** (2014) Kinetics of tracheid development explain
625 conifer tree-ring structure. *New Phytologist* **203**: 1231–1241
- 626 **Cuny HE, Rathgeber CBK, Frank D, Fonti P, Mäkinen H, Prislan P, Rossi S, del Castillo EM, Campelo P, H.**
627 **V, Camarero JJ, Bryukhanova MV, Jyske T, Gričar J, Gryc V, De Luis M, Vieira J, Čufar K,**
628 **Kirdeyanov AV, Oberhuber W, Tremli V, Huang JG, Li X, Swidrak I, Deslauriers A, Liang E, Nöjd P,**
629 **Gruber A, Nabais C, Morin H, Krause C, King G, Fournier M** (2015) Intra-annual dynamics of
630 woody biomass production in coniferous forests. *Nature Plants* **1**: 15160
- 631 **Daudet F-A, Améglio T, Cochard H, Archilla O, Lacoïnte A** (2005) Experimental analysis of the role of
632 water and carbon in tree stem diameter variations. *Journal of Experimental Botany* **56**: 135-144
- 633 **De Schepper V, De Swaef T, Bauweraerts I, Steppe K** (2013) Phloem transport: a review of mechanisms
634 and controls. *Journal of Experimental Botany* **64**: 4839-4850
- 635 **de Schepper V, Steppe K, Van Labeke MC, Lemeur R** (2010) Detailed analysis of double girdling effects
636 on stem diameter variations and sap flow in young oak trees. *Environmental and Experimental*
637 *Botany* **68**: 149-156
- 638 **Deslauriers A, Beaulieu M, Balducci L, Giovannelli A, Gagnon MJ, Rossi S** (2014) Impact of warming and
639 drought on carbon balance related to wood formation in black spruce. *Annals of Botany* **114**:
640 335-345
- 641 **Deslauriers A, Giovannelli A, Rossi S, Castro G, Fragnelli G, Traversi L** (2009) Intra-annual cambial
642 activity and carbon availability in stem of poplar. *Tree Physiology* **29**: 1223-1235
- 643 **Deslauriers A, Morin H, Begin Y** (2003) Cellular phenology of annual ring formation of *Abies balsamea* in
644 Quebec boreal forest (Canada). *Canadian Journal of Forest Research* **33**: 190-200
- 645 **dos Santos TB, Budzinski IGF, Marur CJ, Petkowicz CLO, Pereira LFP, Vieira LGE** (2011) Expression of
646 three galactinol synthase isoforms in *Coffea arabica* L. and accumulation of raffinose and
647 stachyose in response to abiotic stresses. *Plant Physiology and Biochemistry* **49**: 441-448
- 648 **Fatichi S, Leuzinger S, Korner C** (2014) Moving beyond photosynthesis: from carbon source to sink-
649 driven vegetation modeling. *New Phytologist* **201**: 1086-1095
- 650 **Freixes S, Thibaud MC, Tardieu F, Muller B** (2002) Root elongation and branching is related to local
651 hexose concentration in *Arabidopsis thaliana* seedlings. *Plant Cell and Environment* **25**: 1357-
652 1366
- 653 **Gartner B, Baker D, Spicer R** (2000) Distribution and vitality of xylem rays in relation to leaf area in
654 Douglas-fir. *IAWA Journal* **21**: 389-401

655 **Giovannelli A, Emiliani G, Traversi ML, Deslauriers A, Rossi S** (2011) Sampling cambial region and
656 mature xylem for non structural carbohydrates and starch analyses. *Dendrochronologia* **29**: 177-
657 182

658 **Gričar J, Čufar K, Oven P, Schmitt U** (2005) Differentiation of terminal latewood tracheids in silver fir
659 trees during autumn. *Annals of Botany* **95**: 959-965

660 **Gruber A, Strobl S, Veit B, Oberhuber W** (2010) Impact of drought on the temporal dynamics of wood
661 formation in *Pinus sylvestris*. *Tree Physiology* **30**: 490-501

662 **Gruber A, Wieser G, Oberhuber W** (2009) Intra-annual dynamics of stem CO₂ efflux in relation to
663 cambial activity and xylem development in *Pinus cembra*. *Tree Physiology* **29**: 641-649

664 **Hansen J, Beck E** (1990) The fate and path of assimilation products in the stem of 8-year-old Scots pine
665 (*Pinus sylvestris* L.) trees. *Trees: Structure and Function* **4**: 16-21

666 **Hansen J, Beck E** (1994) Seasonal change in the utilization and turnover of assimilation products in 8-
667 year-old Scots pine (*Pinus sylvestris* L.) trees. *Trees: Structure and Function* **8**: 172-182

668 **Harris DC** (1997) Internal Standards. *In* Quantitative chemical analysis, Fifth edition. W.H. Freeman and
669 Company, New York, USA, p 104

670 **Huang J, Bergeron Y, Berninger F, Zhai L, Tardif J, denneler B** (2013) Impact of future climate on radial
671 growth of four major boreal tree species in the eastern Canadian boreal forest. *PLoS ONE* **8**:
672 e56758

673 **Huang J, Deslauriers A, Rossi S** (2014) Xylem formation can be modeled statistically as a function of
674 primary growth and cambium activity. *New Phytologist* **203**: 831-841

675 **Johnson JM, Pritchard J, Gorham J, Tomos AD** (1996) Growth, water relations and solute accumulation
676 in osmotically stressed seedlings of the tropical tree *Colophospermum mopane*. *Tree Physiology*
677 **16**: 713-718

678 **Kagawa A, Sugimoto A, Maximov TC** (2006) ¹³C₂ pulse-labelling of photoassimilates reveals carbon
679 allocation within and between tree rings. *Plant Cell Environ* **29**: 1571-1584

680 **Koch K** (2004) Sucrose metabolism: regulatory mechanisms and pivotal roles in sugar sensing and plant
681 development. *Current Opinion in Plant Biology* **7**: 235-246

682 **Körner C** (2003) Carbon limitation in trees. *Journal of Ecology* **91**: 4-17

683 **Lastdrager J, Hanson J, Smeekens S** (2014) Sugar signals and the control of plant growth and
684 development. *Journal of Experimental Botany* doi:10.1093/jxb/ert474

685 **Lavigne MB, Little CHA, Riding RT** (2004) Changes in stem respiration rate during cambial reactivation
686 can be used to refine estimates of growth and maintenance respiration. *New Phytologist* **162**:
687 81-93

688 **Maier CA, Johnsen KH, Clinton BD, Ludovici KH** (2010) Relationship between stem CO₂ efflux, substrate
689 supply, and growth in young loblolly pine trees. *New Phytologist* **185**: 502-513

690 **Maunoury-Danger F, Fresneau C, Eglin T, Berveiller D, François C, Lelarge-Trouverie C, Damesin C**
691 (2010) Impact of carbohydrate supply on stem growth, wood and respired CO₂ δ¹³C:
692 assessment by experimental girdling. *Tree Physiology* **30**: 818-830

693 **Merlo J, Chaix B, Yang M, Lynch J, Rastam L** (2005) A brief conceptual tutorial on multilevel analysis in
694 social epidemiology: interpreting neighbourhood differences and the effect of neighbourhood
695 characteristics on individual health. *Journal of Epidemiology & Community Health* **59**: 1022-1028

696 **Michelot A, Simard S, Rathgeber C, Dufrêne E, Damesin C** (2012) Comparing the intra-annual wood
697 formation of three European species (*Fagus sylvatica*, *Quercus petraea* and *Pinus sylvestris*) as
698 related to leaf phenology and non-structural carbohydrate dynamics. *Tree Physiology* **32**: 1033-
699 1045

700 **Muller B, Pantin F, Genard M, Turc O, Freixes S, Piques M, Gibon Y** (2011) Water deficits uncouple
701 growth from photosynthesis, increase C content, and modify the relationships between C and
702 growth in sink organs. *Journal of Experimental Botany* **62**: 1715-1729

703 **Nakagawa S, Schielzeth H** (2013) A general and simple method for obtaining R^2 from generalized linear
704 mixed-effects models. *Methods in Ecology and Evolution* **4**: 133-142

705 **Nishizawa-Yokoi A, Yabuta Y, Shigeoka S** (2008) The contribution of carbohydrates including raffinose
706 family oligosaccharides and sugar alcohols to protection of plant cells from oxidative damage.
707 *Plant Signaling and Behavior* **3**: 1016-1018

708 **O'Brien R** (2007) A caution regarding rules of thumb for variance inflation factors. *Quality & Quantity* **41**:
709 673–690

710 **Olano JM, Arzac A, García-Cervigón AI, von Arx G, Rozas V** (2013) New star on the stage: Amount of ray
711 parenchyma in tree rings shows a link to climate. *New Phytologist* **198**: 486-495

712 **Oribe Y, Funada R, Kubo T** (2003) Relationships between cambial activity, cell differentiation and the
713 localization of starch in storage tissues around the cambium in locally heated stem of *Abies*
714 *sachalinensis* (Schmidt) Master. *Trees: Structure and Function* **14**: 185-192

715 **Orthen B, Popp M, Smirnov N** (1994) Hydroxyl radical scavenging properties of cyclitols. *Proceedings of*
716 *the Royal Society of Edinburgh Section B: Biology* **102**: 269-272

717 **Palacio S, Hoch G, Sala A, Korner C, Millard P** (2014) Does carbon storage limit tree growth? *New Phytol*
718 **201**: 1096-1100

719 **Pantin F, Fanciullino AL, Massonnet C, Dauzat M, Simonneau T, Muller B** (2013) Buffering growth
720 variations against water deficits through timely carbon usage. *Front Plant Sci* **4**: 483

721 **Pantin F, Simonneau T, Muller B** (2012) Coming of leaf age: control of growth by hydraulics and
722 metabolics during leaf ontogeny. *New Phytologist* **196**: 349-366

723 **Pinheiro J, Bates D** (2000) *Mixed-effects models in S and S-PLUS*. Springer, New York, USA

724 **Rocha AV** (2013) Tracking carbon within the trees. *New Phytologist* **197**: 685-686

725 **Rossi S, Anfodillo T, Cufar K, Cuny HE, Deslauriers A, Fonti P, Frank D, Gricar J, Gruber A, King GM,**
726 **Krause C, Morin H, Oberhuber W, Prislan P, Rathgeber CBK** (2013) A meta-analysis of cambium
727 phenology and growth: linear and non-linear patterns in conifers of the northern hemisphere.
728 *Annals of Botany* **112**: 1911-1920

729 **Rossi S, Anfodillo T, Menardi R** (2006) Trephor: A new tool for sampling microcores from tree stems.
730 *IAWA Journal* **27**: 89-97

731 **Rossi S, Deslauriers A, Anfodillo T, Morin H, Saracino A, Motta R, Borghetti M** (2006) Conifers in cold
732 environments synchronize maximum growth rate of tree-ring formation with day length. *New*
733 *Phytologist* **170**: 301-310

734 **Rossi S, Deslauriers A, Griçar J, Seo JW, Rathgeber CBK, Anfodillo T, Morin H, Levanic T, Oven P,**
735 **Jalkanen R** (2008) Critical temperatures for xylogenesis in conifers of cold climates. *Global*
736 *Ecology and Biogeography* **17**: 696-707

737 **Rossi S, Simard S, Rathgeber C, Deslauriers A, De Zan C** (2009) Effects of a 20-day-long dry period on
738 cambial and apical meristem growth in *Abies balsamea* seedlings. *Trees - Structure and Function*
739 **23**: 85-93

740 **Scheible WR, Lauerer M, Schulze ED, Caboche M, Stitt M** (1997) Accumulation of nitrate in the shoot
741 acts as a signal to regulate shoot-root allocation in tobacco. *Plant Journal* **11**: 671-691

742 **Schiestl-Aalto P, Kulmala L, Mäkinen H, Nikinmaa E, Mäkelä A** (2015) CASSIA – a dynamic model for
743 predicting intra-annual sink demand and interannual growth variation in Scots pine. *New*
744 *Phytologist* **206**: 647-659

745 **Sevanto S, McDowell NG, Dickman LT, Pangle R, Pockman WT** (2014) How do trees die? A test of the
746 hydraulic failure and carbon starvation hypotheses. *Plant Cell and Environment* **37**: 153-161

747 **Simard S, Giovannelli A, Treydte K, Traversi M, M.King G, Frank D, Fonti P** (2013) Intra-annual dynamics
748 of non-structural carbohydrates in the cambium of mature conifer trees reflects radial growth
749 demands. *Tree Physiology* **33**: 913-923

750 **Singer J** (1998) Using SAS Proc Mixed to fit multilevel models, hierarchical models, and individual growth
751 models. *Journal of Educational and Behavioral Statistics* **24**: 323-355
752 **Spicer R, Holbrook N** (2007) Parenchyma cell respiration and survival in secondary xylem: does
753 metabolic activity decline with cell age? *Plant, Cell and Environment* **30**: 934-943
754 **Steppe K, Sterck F, Deslauriers A** (2015) Diel growth dynamics in tree stems: linking anatomy and
755 ecophysiology. *Trends in Plant Science* **20**: 335-343
756 **Tardieu F, Granier C, Muller B** (2011) Water deficit and growth. Co-ordinating processes without an
757 orchestrator? *Current Opinion in Plant Biology* **14**: 283-289
758 **Turnbull MH, Tissue DT, Murthy R, Wang XZ, Sparrow AD, Griffin KL** (2004) Nocturnal warming
759 increases photosynthesis at elevated CO₂ partial pressure in *Populus deltoides*. *New Phytologist*
760 **161**: 819-826
761 **Way DA, Sage RF** (2008) Elevated growth temperatures reduce the carbon gain of black spruce *Picea*
762 *mariana* (Mill.) BSP. *Global Change Biology* **14**: 624-636
763 **Wiley E, Helliker B** (2012) A re-evaluation of carbon storage in trees lends greater support for carbon
764 limitation to growth. *New Phytologist* **195**: 285-289
765 **Wolfgang H** (1985) Seasonal fluctuation of reserve materials in the trunkwood of spruce (*Picea abies*
766 (L.) Karst.). *Journal of Plant Physiology* **117**: 355-362
767 **Woodruff DR** (2014) The impacts of water stress on phloem transport in Douglas-fir trees. *Tree*
768 *Physiology* **34**: 5-14
769 **Woodruff DR, Meinzer FC** (2011) Water stress, shoot growth and storage of non-structural
770 carbohydrates along a tree height gradient in a tall conifer. *Plant Cell and Environment* **34**: 1920-
771 1930
772
773